Phonon-self-energy effects due to an electronic mechanism in high-T_c superconductors

E. J. Nicol* and J. P. Carbotte
Department of Physics and Astronomy, McMaster University, Hamilton, Ontario, Canada L8S 4M1
(Received 17 July 1992)

The phonon self-energy at $\mathbf{q}=\mathbf{0}$ and zero temperature is calculated for a conventional electron-phonon superconductor, Pb, and for an equivalent high-T_c superconductor, assuming an electronic mechanism for the superconductivity (to be specific and as a convenient illustrative example, we use the marginal-Fermi-liquid phenomenology). Comparison between the results demonstrates that for an s-wave strong-coupling superconductor, phonon shifts and widths exhibit the same behavior regardless of the mechanism for superconductivity. In addition, the marginal-Fermi-liquid model shows no unusual behavior at zero temperature in the phonon self-energy, with the exception of a possible narrowing of the phonon width below $2\Delta_0$ in the clean limit. As an aside, we also present renormalized BCS formulas that agree well with the full numerical strong-coupling calculations and could be easily implemented for use in model fits.

I. INTRODUCTION

Raman light-scattering experiments have been a valuable tool in the field of superconductivity for their potential to comment on various issues.[1,2] For instance, in the normal state, the Raman intensity is related to the normal-state conductivity and therefore provides an image of the excitations in the system. The Raman intensity is also simply related to the absorptive part of the polarizability and has been used to motivate the marginal-Fermi-liquid phenomenology for high-temperature superconductivity which is based on an assumed form of the absorptive part of the polarizability.[3] The superconducting state will also be manifested in these experiments by removal of electronic states from below $\omega=2\Delta$, where Δ is the energy gap, to a pileup of the same just above 2Δ.[1] In addition, Raman-active phonons observed in these experiments will broaden or narrow, and shift up or down in frequency as the sample changes from the normal to the superconducting state, depending on the energy of the phonon with respect to the gap energy.[4] Hence, Raman experiments can be a very useful probe of the superconducting state. Many reviews exist on this subject which expand further on these and related topics.[1,2]

In this paper, we would like to focus on the superconductivity-induced phonon self-energy effects of the $\mathbf{q}=\mathbf{0}$ phonons. This quantity was calculated by Zeyher and Zwicknagl[4] for the high-temperature superconductors and has become very popular for analyzing the data in terms of an energy gap.[5-9] Our purpose here is twofold. First, we would like to ask the question: Can the phonon self-energy effects tell us about the mechanism, i.e., can an electron-phonon mechanism for superconductivity be distinguished from an electronic one? Second, the question has been asked several times, what does the marginal-Fermi-liquid phenomenology do to the phonon self-energy in the superconducting state? Will it be ruled out in this experiment?

In addition, we will give simple renormalized BCS formulas that can be used in lieu of the Zeyher-Zwicknagl theory for experimental fitting for strong-coupling effects without the need for the full numerical machinery of strong-coupling Eliashberg theory. This could be of use to experimentalists.

II. THEORY

In their paper, Zeyher and Zwicknagl[4] have given a detailed discussion of the phonon self-energy effects in the high-T_c oxides. They have also given detailed arguments for using the lowest-order approximation for the phonon self-energy diagram. Normally, the phonon self-energy effects for the $\mathbf{q}=0$ phonons will be zero due to Coulomb effects,[10] however, for the B_{1g} mode, the Coulomb effects drop out of the problem and the phonon self-energy effects can be observed in this case. Because of this, the vertex corrections can be neglected and the superconductivity-induced polarization to lowest order is all that need be calculated.[4]

Under the assumption that the electron-phonon coupling is independent of momentum, the phonon self-energy is proportional to the polarization bubble diagram shown in Fig. 1. For $\mathbf{q}=0$ the polarization $\Pi(i\nu_n)$ is written in terms of the boson and fermion Matsubara frequencies, $i\nu_n$ and $i\omega_m$, respectively, as[4,11]

$$\Pi(i\nu_n) = \frac{1}{N\beta}\sum_{\mathbf{k},i\omega_m} \mathrm{Tr}\{\hat{\tau}_3\hat{G}(\mathbf{k},i\omega_m+i\nu_n)\hat{\tau}_3\hat{G}(\mathbf{k},i\omega_m)\}\ . \quad (1)$$

Here, N is the number of lattice sites, β is the inverse temperature, $\hat{\tau}_3$ is the usual Pauli matrix, and $\hat{G}(\mathbf{k},i\omega_m)$

FIG. 1. The polarization diagram in the lowest-order approximation (i.e., with no vertex corrections) as discussed in the text.

is the electron Green's function, given in the superconducting state as[11,12]

$$\hat{G}(\mathbf{k},i\omega_m)=-\frac{i\tilde{\omega}_m+\epsilon_k\hat{\tau}_3+\tilde{\Delta}(i\omega_m)\hat{\tau}_1}{\tilde{\omega}_m^2+\epsilon_k^2+\tilde{\Delta}^2(i\omega_m)} . \quad (2)$$

If the sum over $\mathbf{k}$ is converted to an integral over energy, assuming a constant density of states in the standard approximation, one obtains for the difference between the superconducting state and the normal state, $\Delta\Pi(i\nu_n)\equiv\Pi^S(i\nu_n)-\Pi^N(i\nu_n)$:

$$\frac{\Delta\Pi(i\nu_n)}{N(0)}=2\pi T\sum_{m=-\infty}^{\infty}\frac{1}{\sqrt{\tilde{\omega}_m^2+\tilde{\Delta}_m^2}+\sqrt{\tilde{\omega}_{m+n}^2+\tilde{\Delta}_{m+n}^2}}\left\{1-\frac{\tilde{\omega}_m\tilde{\omega}_{m+n}+\tilde{\Delta}_m\tilde{\Delta}_{m+n}}{\sqrt{\tilde{\omega}_m^2+\tilde{\Delta}_m^2}\sqrt{\tilde{\omega}_{m+n}^2+\tilde{\Delta}_{m+n}^2}}\right\}$$
$$-2\pi T\sum_{m=-\infty}^{\infty}\frac{1}{\tilde{\omega}_m^0+\tilde{\omega}_{m+n}^0}\{1-\mathrm{sgn}(\tilde{\omega}_m^0\tilde{\omega}_{m+n}^0)\} . \quad (3)$$

Here the superscript 0 refers to $\tilde{\omega}$ evaluated in the normal state. Notice that the normal state [resulting from setting $\tilde{\Delta}=0$ in Eqs. (1) and (2)] has been subtracted off for reasons of convergence and to achieve the correct limit as $\nu\to\infty$. This quantity is analytically continued using Padé approximants[13–15] as was done in Ref. 4. Marsiglio, Akis, and Carbotte[11] have done an exact analytic continuation of this quantity and have shown which features in the previous results are artifacts of the Padé approximants scheme. At zero temperature, Padé approximants work reasonably well as we will discuss later.

Finally, we require the Matsubara pairing energy $\tilde{\Delta}(i\omega_n)$ and renormalized frequencies $\tilde{\omega}(i\omega_n)$, which come from a solution of the standard Eliashberg equations on the imaginary axis:[16–18]

$$\tilde{\Delta}_n=\pi T\sum_m[\lambda^-(n-m)-\mu^*(\omega_c)]\frac{\tilde{\Delta}_m}{\sqrt{\tilde{\omega}_m^2+\tilde{\Delta}_m^2}} \quad (4)$$

and

$$\tilde{\omega}_n=\omega_n+\pi T\sum_m\lambda^+(n-m)\frac{\tilde{\omega}_m}{\sqrt{\tilde{\omega}_m^2+\tilde{\Delta}_m^2}} . \quad (5)$$

In Eqs. (4) and (5), $\tilde{\Delta}$ and $\tilde{\omega}$ are related to the gap Δ and renormalization factor Z by $\tilde{\Delta}(i\omega_n)\equiv\Delta(i\omega_n)Z(i\omega_n)$ and $\tilde{\omega}(i\omega_n)\equiv\omega_n Z(i\omega_n)$. The function $\lambda^{\pm}(n-m)$ is related to the electron-phonon spectra density $\alpha^2F(\Omega)$ by

$$\lambda^{\pm}(n-m)=\int_0^{\infty}\frac{2\Omega\alpha^2F(\Omega)}{\Omega^2+(\omega_n-\omega_m)^2}d\Omega , \quad (6)$$

and to the marginal-Fermi-liquid phenomenology by

$$\lambda^{\pm}(n-m)=(\lambda_\rho\pm\lambda_\rho)\int_{2\Delta(T)}^{\omega_0}\frac{2\Omega\tanh(\Omega/2T)}{\Omega^2+(\omega_n-\omega_m)^2}d\Omega . \quad (7)$$

Details of the implementation of the marginal-Fermi-liquid model can be found in Refs. 19–23. Here, λ_ρ (λ_σ) is the coupling to charge (spin) fluctuations and ω_0 is an ultraviolet cutoff. Finally, μ^* is a Coulomb pseudopotential with a cutoff ω_c. This parameter is taken to be zero in the marginal-Fermi-liquid case.

We would like to emphasize at this point that we have chosen to use the marginal-Fermi-liquid model for the electronic mechanism in these equations both for its apparent successes and as it is the most unusual in this class. However, any other form of electronic mechanism would be equally valid and give the same results. The marginal-Fermi-liquid model has the added feature of a lower cutoff in the spectrum at $2\Delta_0$ in the superconducting state, which we impose as a sharp cutoff for simplicity. This feature gives rise to a rapidly falling quasiparticle damping rate in the superconducting state,[24] a $4\Delta_0$ absorption edge in the finite-frequency optical conductivity,[20,22] and a peak in the low-frequency temperature-dependent conductivity.[24,25] As we will see it results in no anomalous behavior in the phonon self-energy at zero temperature. While a cutoff imposed in this crude manner possibly violates the sum rules for the charge part of the interaction,[26] the suppression of the low-frequency behavior in the superconducting state, which in the normal state gives rise to the marginal-Fermi-liquid behavior, signals a restoration of the full quasiparticle nature and a possible return to Fermi-liquid behavior allowing for the use of Fermi-liquid-based theories for the superconducting state. Anderson believes that while there is a sharp increase in the quasiparticle lifetime, Fermi-liquid character is not being restored in the superconducting state.[27]

The marginal-Fermi-liquid model has had success in explaining many of the normal-state properties of the high-T_c oxides.[3] In the superconducting state it also shows promise. There can be a large $2\Delta/k_BT_c$ with little associated Holstein structure in the optical conductivity.[20] The temperature dependence of the penetration depth can fall near the observed two-fluid model behavior.[21] However, one recent set of data has indicated instead a $(1-t^2)$ law, with t the reduced temperature, which would conflict with the marginal-Fermi-liquid model and favor d-wave superconductivity.[28] A peak in the temperature dependence of the microwave conductivity can exist with no corresponding peak in the NMR relaxation rate.[24,25] However, no quantitative fit to both sets of data with a common set of parameters has ever been tried. There is a very rapidly decreasing scattering rate as a function of decreasing temperature in the superconducting state.[24,29,30] Such data is, however, consistent with any mechanism in which the fluctuation spectrum becomes gapped and is not a conclusive proof of marginal-Fermi-liquid behavior. And finally, there is

structure in the quasiparticle density of states at 3Δ as observed in the angular resolved photoemission spectrum,[22,31,32] although the magnitude of the predicted structure is much smaller than is observed. Alternative interpretations of the photoemission data have been advanced.[33,34]

In this paper, we use the marginal-Fermi-liquid model mainly as an explicit example of an electronic mechanism which has been widely discussed in the literature and which we use to illustrate an important point, namely, that the present Raman data on phonon shifts is not inconsistent with an electronic mechanism. We believe that the results are not significantly affected by the choice of electronic mechanism.

The procedure is then to iterate Eqs. (4) and (5) for the renormalized frequencies and gaps, substitute these into Eq. (3), and analytically continue this quantity to the real axis ($i\nu_n \rightarrow \nu + i\delta$) by Padé approximants. The final result $\Delta\Pi(\nu+i\delta)$ is related to the difference between the superconducting and normal-state self-energy, the real part of which corresponds to phonon frequency shifts and the imaginary part to changes in the phonon widths. Our calculations have been done at $T/T_c = 0.1$ which is effectively zero temperature.

We will now summarize our results. First, we will compare the Padé approximant scheme with the exact analytic BCS results, as we will be using Padé approximants for the marginal-Fermi-liquid model calculations shown here. Second, we will present renormalized BCS formulas (these do not apply to the marginal-Fermi-liquid model), demonstrating their level of accuracy by comparison with exact calculations for Pb. And finally we will discuss the results for the marginal-Fermi-liquid model.

III. RESULTS

In Figs. 2(a) and 2(b), we show the BCS result for the real and imaginary parts of the phonon self-energy to illustrate the difference between the Padé approximants and the exact BCS result. The solid curve corresponds to the exact analytic solution of the unrenormalized BCS limit of $\Delta\Pi$ at $T=0$.[4,11] In general, the agreement is quite good at zero temperature with only a slight smearing around the singularity at $2\Delta_0$ in the imaginary part and a slight oscillation above $2\Delta_0$ in the real part. This is due to the difficulty that Padé approximants have in capturing sharp features or singularities. In a $\lambda^{\theta\theta}$ model[12] calculation, where the approximation $\lambda(n-m) = \lambda\theta(\omega_D - |\omega_m|)\theta(\omega_D - |\omega_n|)$ is made, we find that Eq. (1) leads to the *renormalized* BCS result at $T=0$:

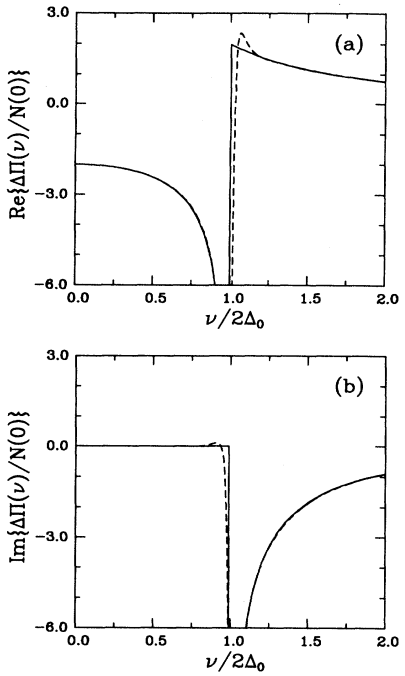

FIG. 2. The phonon self-energy, (a) real and (b) imaginary parts in BCS theory, at zero temperature and in the clean limit. The solid curve is the exact analytic result and the dashed curve is the Padé approximant result. Negative (positive) values correspond to (a) softening (hardening), (b) broadening (sharpening).

$$\frac{\mathrm{Re}\Delta\Pi(\nu+i\delta)}{N(0)} = \begin{cases} -\dfrac{2}{(1+\lambda)\bar{\nu}\sqrt{1-\bar{\nu}^2}}\tan^{-1}\left[\dfrac{\bar{\nu}}{\sqrt{1-\bar{\nu}^2}}\right] & \text{for } \bar{\nu}<1 \\ \dfrac{1}{(1+\lambda)\bar{\nu}\sqrt{\bar{\nu}^2-1}}\ln(2\bar{\nu}^2-1+2\bar{\nu}\sqrt{\bar{\nu}^2-1}) & \text{for } \bar{\nu}>1\ , \end{cases} \tag{8}$$

$$\frac{\mathrm{Im}\Delta\Pi(\nu+i\delta)}{N(0)} = \begin{cases} 0 \quad \text{for } \bar{\nu}<1 \\ -\pi\dfrac{1}{(1+\lambda)\bar{\nu}\sqrt{\bar{\nu}^2-1}} \quad \text{for } \bar{\nu}>1\ , \end{cases} \tag{9}$$

where $\bar{\nu} \equiv \nu/(2\Delta_0)$ and λ is the electron-boson mass renormalization parameter. The unrenormalized BCS results plotted in Figs. 2(a) and 2(b) correspond to $\lambda=0$ in Eqs. (8) and (9). This renormalized BCS result could be useful for quick estimates and fits of the data for strong-coupling effects. We have found by comparing the above formula with exact numerical strong-coupling calculations that the agreement for large λ is not very good quantitatively for $\nu > 2\Delta$ but virtually exact for $\nu < 2\Delta$. With impurity scattering the renormalized BCS result at any temperature T is given as

$$\frac{\Delta\Pi(\nu+i\delta)}{N(0)}=\frac{1}{1+\lambda}\left\{\int_0^\infty d\omega\tanh\frac{\beta\omega}{2}\,\frac{1-N(\omega)N(\omega+\nu)-P(\omega)P(\omega+\nu)}{\epsilon(\omega)+\epsilon(\omega+\nu)+i/[\tau(1+\lambda)]}\right.$$
$$+\int_0^\infty d\omega\tanh\frac{\beta(\omega+\nu)}{2}\,\frac{1-N^*(\omega)N^*(\omega+\nu)-P^*(\omega)P^*(\omega+\nu)}{\epsilon^*(\omega)+\epsilon^*(\omega+\nu)-i/[\tau(1+\lambda)]}$$
$$+\int_0^\infty d\omega\left[\tanh\frac{\beta(\omega+\nu)}{2}-\tanh\frac{\beta\omega}{2}\right]\frac{1-N^*(\omega)N(\omega+\nu)-P^*(\omega)P(\omega+\nu)}{\epsilon(\omega+\nu)-\epsilon^*(\omega)+i/[\tau(1+\lambda)]}$$
$$+\int_{-\nu}^0 d\omega\tanh\frac{\beta(\omega+\nu)}{2}\left[\frac{1-N^*(\omega)N^*(\omega+\nu)-P^*(\omega)P^*(\omega+\nu)}{\epsilon^*(\omega)+\epsilon^*(\omega+\nu)-i/[\tau(1+\lambda)]}\right.$$
$$\left.\left.+\frac{1+N^*(\omega)N(\omega+\nu)+P^*(\omega)P(\omega+\nu)}{\epsilon(\omega+\nu)-\epsilon^*(\omega)+i/[\tau(1+\lambda)]}\right]-\frac{2\nu}{\nu+i/[\tau(1+\lambda)]}\right\},\tag{10}$$

where $\epsilon(\omega)=\sqrt{\omega^2-\Delta^2}$, $N(\omega)=\omega/\epsilon(\omega)$, and $P(\omega)=\Delta/\epsilon(\omega)$. In Figs. 3(a) and 3(b), we test this formula at $T=0$ against the full strong-coupling calculation done on the real axis[11] (no Padé approximants) for Pb with some impurity scattering. The agreement is very good. The virtue of the renormalized formula in this case is that its simple application gives almost exactly the full numerical results without the need for computer intensive calculations. The Padé approximants for this case gave anomalous structure and hence were unreliable. As before, the agreement for $\nu>2\Delta_0$ is not as good. Presumably strong-coupling effects not captured by the simple approximation are coming into play. However, for $\nu<2\Delta_0$ the curve is entirely due to the normal state, where the $\lambda^{\theta\theta}$ model is particularly well suited. Good agreement also occurs at finite temperature.

Having demonstrated the limitations and justified our use of Padé approximants, we now proceed to the results of our calculation of interest. In Figs. 4(a) and 4(b), we show the real and imaginary parts of the phonon self-energy. The solid curve is for the marginal-Fermi-liquid model with the following parameters: $\omega_0=200$ meV,

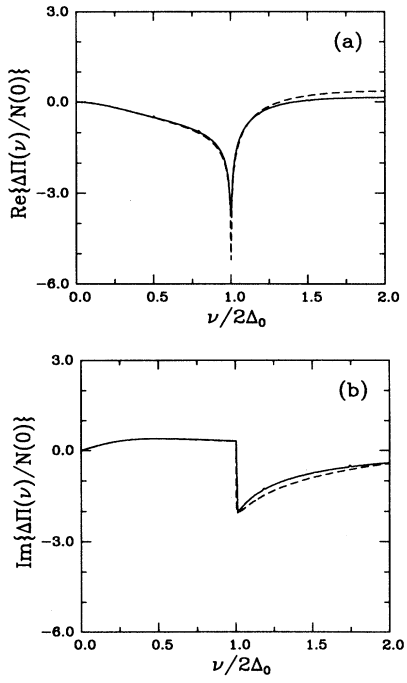

FIG. 3. The phonon self-energy, (a) real and (b) imaginary parts for Pb with $1/\tau=2.16$ meV (dashed curve). The exact real-axis strong-coupling calculation has been done using the tunneling-derived $\alpha^2F(\omega)$ spectrum for Pb. This is compared with the renormalized BCS formula in Eq. (10) using the λ for Pb, which is 1.55, and $T=0$ (solid curve). The agreement between the two curves is very good, illustrating the usefulness of the simpler formula given in Eq. (10).

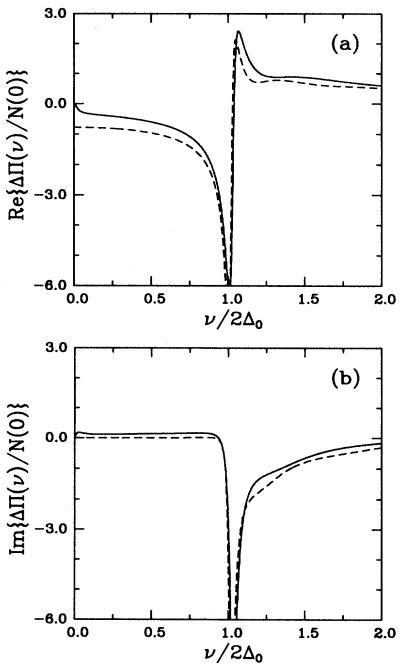

FIG. 4. The phonon self-energy, (a) real and (b) imaginary parts for Pb (dashed curve) and for the marginal-Fermi-liquid model (solid curve), both in the clean limit and for $T/T_c=0.1$. Parameters are given in the text. Note that there is essentially no appreciable difference between an electronic mechanism and an electron-phonon one. Negative (positive) values correspond to (a) softening (hardening), (b) broadening (sharpening).

$g=(\lambda_\rho-\lambda_\sigma)/(\lambda_\rho+\lambda_\sigma)=0.8$, $T_c=100$ K, $2\Delta_0/k_BT_c=4.55$, $\Delta_0=19.6$ meV, $\lambda\sim1.3$, and $\mu^*=0$ (see Ref. 24 for details). The dashed curve is for the tunneling derived $\alpha^2F(\omega)$ spectrum of Pb. The characteristics of Pb are $T_c=7.19$ K, $2\Delta_0/k_BT_c=4.49$, $\Delta_0=1.39$ meV, $\lambda=1.55$, and $\mu^*=0.139$.[18] The marginal-Fermi-liquid model was chosen to have strong-coupling parameters, $2\Delta_0/k_BT_c$ and λ, similar to Pb so that a comparison between the two mechanisms could be made independent of strong-coupling behavior. According to Fig. 4(a), a phonon with frequency below $2\Delta_0$ would soften while one above $2\Delta_0$ would harden; this is similar to the BCS result in Fig. 2(a) but lesser in magnitude. Note that the oscillations above $2\Delta_0$ are a result of the Padé approximant scheme. In the exact analytic continuation scheme there would be a sharp cusp as in Fig. 2(a). (This should have been the case in Ref. 11, however, the numerical integration was not sufficiently accurate and the cusp feature was rounded instead.) The primary result is that the two models give qualitatively and almost quantitatively the same result. It is clear that the observed pattern of behavior for phonon shifts cannot be used to differentiate between electron-phonon and electronic models. Both are consistent with present data. It should be pointed out, however, that the absolute value of observed shifts depends on the electron-phonon coupling constant squared ($|g_{\lambda kk'}|^2$), a quantity which would be expected to be quite different for a phonon model and a marginal-Fermi-liquid model. We have not treated this difficult problem here as this would go beyond the present scope of this work and such an analysis would probably be worthwhile only after the marginal-Fermi-liquid model is more firmly established and a microscopic derivation forthcoming. Neither of these criteria have yet been met.

Likewise, in Fig. 4(b), for the phonon widths, a phonon with frequency less than $2\Delta_0$ neither narrows nor broadens in the superconducting state because no scattering can occur while above $2\Delta_0$ it broadens. Again the two models are almost indistinguishable with the exception of $\nu<2\Delta_0$. To comment on the quantitative difference in these figures, we must point out two items. First, in the procedure of gapping the marginal-Fermi-liquid spectrum at low frequency, we have not accounted for the loss in spectral weight and hence in the difference between the superconducting and normal states there would be a positive shift in $\Delta\Pi$. This would be negligible. Also, in the normal state of the marginal Fermi liquid, the spectrum goes to zero frequency as ω instead of as ω^2 in the case of Pb or any other phonon spectrum. Hence, this strong-coupling weight at low frequency has an effect of acting like static impurities. It is well known from functional derivative calculations for superconducting properties that are affected by impurities[35,36] that very low-frequency phonons ($\omega/T_c\ll1$) mimic static impurity scattering. In this case, we are looking only at the clean limit, but previous work[11] has also shown that with the addition of impurities Π^N is finite and hence the slightly positive direction of the $\mathrm{Im}\Delta\Pi$ below $2\Delta_0$ is due to this (Π^s being zero below $\nu=2\Delta_0$). We will comment further on this shortly.

As an aside to this discussion, it was not commented on in Ref. 11 that $\mathrm{Im}\Delta\Pi$ for $\omega<2\Delta_0$ was slightly positive in the extreme strong-coupling case partly for the same reasons as given above. The best strong-coupling parameter is $T_c/\omega_{\ln}$, where $\omega_{\ln}$ is some average frequency of the $\alpha^2F(\omega)$ spectrum.[18,37] $T_c/\omega_{\ln}\to0$ corresponds to the BCS weak-coupling limit and $T_c/\omega_{\ln}\gg1$ is extreme strong coupling. The $T_c/\omega_{\ln}$ for Pb is 0.128. Hence for very strong coupling $T_c/\omega_{\ln}\gg1$ or, alternatively, $\omega_{\ln}/T_c\ll1$ and, as discussed above, in this limit phonons are beginning to behave like static impurities.

To address the question of whether the slight sharpening below $2\Delta_0$ is a real feature of the marginal-Fermi-liquid model, we show in Figs. 5(a) and 5(b) the marginal-Fermi-liquid model for two cases: gapped and ungapped. In the latter case, the same marginal-Fermi-liquid model is employed as previously discussed but there is no low-frequency gapping of the fluctuation spectrum, i.e., the lower limit on the integral in Eq. (7) is set to zero. In this ungapped case, the strong-coupling parameters are higher and we notice that the gapped model (dashed curve) agrees well at low frequency with the ungapped case (solid curve), and hence the gapped case seems to retain a memory of its ungapped version. This can easily be understood from the fact that below $2\Delta_0$ only the normal-state contributes; therefore there is the return to the ungapped (normal-state) model in this region. Hence, the shift upwards in the curves in Fig. 4 compared with that of Pb is a result of this memory. Also the gapped case looks very similar to a renormalized

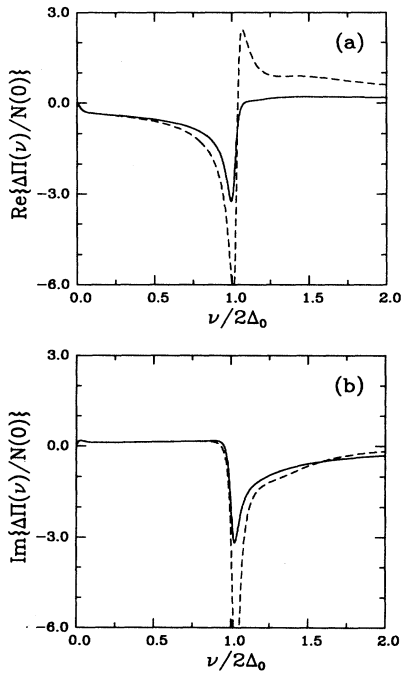

FIG. 5. The phonon self-energy, (a) real and (b) imaginary parts for the marginal-Fermi-liquid model in the ungapped case (solid curve) and the gapped case (dashed curve) in the clean limit and for $T/T_c=0.1$.

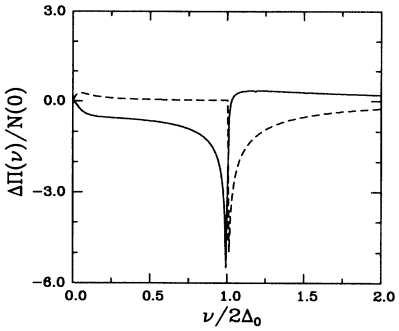

FIG. 6. The phonon self-energy, real (solid curve) and imaginary (dashed curve) parts calculated from the renormalized BCS formula at $T=0$ and with $1/[(1+\lambda)\tau\Delta_0]=0.1$. The similarity between these curves and those of the ungapped case of the marginal-Fermi-liquid model in Fig. 5 is striking.

BCS curve with a small amount of impurities. To illustrate this we used Eq. (10) with the appropriate λ for the ungapped case and $1/[(1+\lambda)\tau\Delta_0]=0.1$, and have plotted the result in Fig. 6. There clearly is a similarity of the results of the ungapped marginal-Fermi-liquid model in Fig. 5 to impurity scattering shown in Fig. 6. The similarity is so strong that it reinforces our previous conclusion that the $\sim\omega$ dependence in the fluctuation spectrum at low frequencies is acting as static impurity scattering. Therefore, the slight sharpening of a phonon with energy $\nu<2\Delta_0$ in the clean-limit version of the marginal-Fermi-liquid model of Fig. 4 appears to be a real feature of this model. However, it would be difficult to distinguish this from regular impurity scattering in an electron-boson model, making this more of a theoretical point of difference rather than an experimentally verifiable feature of a marginal-Fermi liquid.

IV. CONCLUSIONS

To summarize, we have calculated the phonon self-energy for the conventional strong-coupling superconductor Pb and compared it with a similar calculation done for an electronic model for the mechanism of the high-T_c superconductors (namely, the marginal-Fermi-liquid model). Our main conclusion is, for different mechanisms with the same strong-coupling effects in an isotropic s-wave superconductor, the phonon self-energy is essentially the same. Hence, it is not possible to distinguish between the electron-phonon mechanism and some other bosonic mechanism for an s-wave superconductor. Thus, while the Zeyher and Zwicknagl theory may be used to extract a possible energy gap from the data, there is no proof that this is an electron-phonon mechanism and other experiments seem to rule otherwise.[38] However, it will be shown in another publication[39] that the nature of the gap parameter with regard to anisotropy will have qualitatively different behavior than discussed here and elsewhere.

In this work, we have examined only the clean limit. We have also calculated the same models with normal impurity scattering and have found the standard behavior as reported previously,[4,11] with no difference between the two mechanisms studied here.

It should also be noted that we have not attempted to do calculations at finite temperature in the superconducting state. These calculations require the use of an exact analytic continuation of the phonon self-energy[11] and within the marginal-Fermi-liquid model such a calculation is numerically intensive. While a finite-temperature calculation could be of significant interest for the marginal-Fermi-liquid model which has a temperature-dependent kernel, there is no microscopic theory for the development of the low-frequency gap in the spectrum of excitations. Therefore, a finite-temperature calculation would also involve examining several possible models for the development of the gap for reasonable statements to be made and it is not deemed to be worth the numerical effort at this time.

One final point to be made in this regard is that the polarization calculated here is similar to that for the optical conductivity, with the Pauli matrices at the vertex giving rise to different coherence factors in the two cases.[11] The superconducting state optical conductivity in the marginal-Fermi-liquid phenomenology shows zero absorption until $\omega=4\Delta_0$ in the clean limit, but the phonon self-energy shows no such anomalous features, with the exception of a possible sharpening below $2\Delta_0$. The phonon self-energy at $\mathbf{q}=0$ is a measure of the existence of a superconducting energy gap and the structure of the gap parameter.

We have also presented renormalized BCS formulas which we hope would be useful to experimentalists for model fits for strong-coupling effects. These formulas are easily implemented and agree reasonably well with the full numerical strong-coupling calculations.

ACKNOWLEDGMENTS

We would like to thank M. Reedyk and F. Marsiglio for helpful discussions. This work was partly supported by the Natural Sciences and Engineering Research Council of Canada (NSERC) and by the Canadian Institute for Advanced Research (CIAR).

*Present address: Department of Physics, University of California, Santa Barbara, CA 93106-9530.

[1]M. Cardona, in *Proceedings of the International Conference on High T_c Superconductivity–ICSC,* edited by S. K. Joshi, C. N. R. Rao, and S. V. Subramanyam (World Scientific, Singapore, 1990), p. 208.

[2]M. Cardona, Physica C **185-189**, 65 (1991), and references to reviews therein.

[3]C. M. Varma, P. B. Littlewood, S. Schmitt-Rink, E. Abrahams, and A. Ruckenstein, Phys. Rev. Lett. **63**, 1996 (1989); **64**, 497(E) (1990).

[4]R. Zeyher and G. Zwicknagl, Solid State Commun. **66**, 617 (1988); Z. Phys. B **78**, 175 (1990).

[5]B. Friedl, C. Thomsen, and M. Cardona, Phys. Rev. Lett. **65**, 915 (1990).

[6]C. Thomsen, M. Cardona, B. Friedl, C. O. Rodriguez, I. I. Ma-

zin, and O. K. Anderson, Solid State Commun. **75**, 219 (1990).
[7]E. Altendorf, J. Chrzanowski, and J. C. Irwin, Physica C **175**, 47 (1991).
[8]K. F. McCarty, H. B. Radousky, J. Z. Liu, and R. N. Shelton, Phys. Rev. B **43**, 13 751 (1991).
[9]S. L. Cooper, M. V. Klein, B. G. Pazol, J. P. Rice, and D. M. Ginsberg, Phys. Rev. B **37**, 5920 (1988).
[10]P. B. Littlewood and C. M. Varma, Phys. Rev. B **26**, 4883 (1982).
[11]F. Marsiglio, R. Akis, and J. P. Carbotte, Phys. Rev. B **45**, 9865 (1992).
[12]P. B. Allen and B. Mitrović, Solid State Phys. **37**, 1 (1982).
[13]H. J. Vidberg and J. W. Serene, J. Low Temp. Phys. **29**, 179 (1977).
[14]C. R. Leavens and D. S. Ritchie, Solid State Commun. **53**, 137 (1985).
[15]R. Blaschke and R. Blocksdorf, Z. Phys. B **49**, 99 (1982).
[16]D. Rainer and G. Bergmann, J. Low Temp. Phys. **14**, 501 (1974).
[17]J. M. Daams and J. P. Carbotte, J. Low Temp. Phys. **43**, 263 (1981).
[18]J. P. Carbotte, Rev. Mod. Phys. **62**, 1027 (1990).
[19]Y. Kuroda and C. M. Varma, Phys. Rev. Lett B **42**, 8619 (1990).
[20]E. J. Nicol, J. P. Carbotte, and T. Timusk, Phys. Rev. B **43**, 473 (1991); Solid. State Commun. **76**, 937 (1990).
[21]E. J. Nicol and J. P. Carbotte, Phys. Rev. B **43**, 1158 (1991).
[22]P. B. Littlewood and C. M. Varma, J. Appl. Phys. **69**, 4979 (1991).
[23]P. B. Littlewood (unpublished).
[24]E. J. Nicol and J. P. Carbotte, Phys. Rev. B **44**, 7741 (1991).
[25]M. C. Nuss, P. M. Mankiewich, M. L. O'Malley, E. H. Westerwick, and P. B. Littlewood, Phys. Rev. Lett. **66**, 3305 (1991).
[26]A. J. Leggett (private communication).
[27]P. W. Anderson, Phys. Rev. B **42**, 2624 (1990); (private communication).
[28]D. A. Bonn, Ruixing Liang, T. M. Riseman, D. J. Baar, D. C. Morgan, Kuan Zhang, P. Dosanjh, T. L. Duty, A. MacFarlane, G. D. Morris, J. H. Brewer, W. N. Hardy, C. Kallin, and A. J. Berlinsky, Phys. Rev. B (to be published).
[29]D. B. Romero, C. D. Porter, D. B. Tanner, L. Forro, D. Mandrus, L. Mihaly, G. L. Carr, and G. P. Williams, Phys. Rev. Lett. **68**, 1590 (1992).
[30]D. A. Bonn, P. Dosanjh, R. Liang, and W. N. Hardy, Phys. Rev. Lett. **68**, 2390 (1992).
[31]D. S. Dessau *et al.*, Phys. Rev. Lett. **66**, 2160 (1991).
[32]Y. Hwu *et al.*, Phys. Rev. Lett. **67**, 2573 (1991).
[33]G. B. Arnold, F. M. Mueller, and J. C. Swihart, Phys. Rev. Lett. **67**, 2569 (1991).
[34]J. C. Phillips, Physica C **195**, 239 (1992).
[35]F. Marsiglio, M. Schossmann, E. Schachinger, and J. P. Carbotte, Phys. Rev. B **35**, 3226 (1987).
[36]E. J. Nicol and J. P. Carbotte, Phys. Rev. B **43**, 10 210 (1991).
[37]P. B. Allen and R. C. Dynes, Phys. Rev. B **12**, 905 (1975).
[38]For instance, Z. Schlesinger, R. T. Collins, F. Holtzberg, C. Field, N. E. Bickers, and D. J. Scalapino, Nature **343**, 242 (1990).
[39]E. J. Nicol, C. Jiang, and J. P. Carbotte, this issue, Phys. Rev. B **47**, 8131 (1993).